Int. J. Electrochem. Sci., 8 **(2013)** 11264 - 11277

International Journal of
ELECTROCHEMICAL
SCIENCE
www.electrochemsci.org

A Novel Sensor of Quinazolin Derivative Self-Assembled Monolayers over Silver Nanoparticles for the Determination of Hydroxylamine

Navid Nasirizadeh[1,2,*], *M. Mehdi Aghayizadeh*[1], *S. Mansour Bidoki*[2], *M. Esmail Yazdanshenas*[1]

[1]Department of Textile Engineering, Yazd Branch, Islamic Azad University, Yazd, Iran
[2]Scientific Society of Nanotechnology, Yazd Branch, Islamic Azad University, Yazd, Iran
[3]Department of Textile, Yazd University, Yazd, Iran
[*]E-mail: nasirizadeh@yahoo.com

Received: 11 June 2013 / *Accepted:* 19 July 2013 / *Published:* 20 August 2013

The electrochemical study of a quinazolin silver nanoparticles−modified glassy carbon electrode (QMSNPs−GCE) as well as its efficacy for electrocatalytic oxidation of hydroxylaminein presence of such self−assembled monolayer (SAM) modified electrodeis described. The QMSNPs−GCE demonstrated a highly catalytic activity in hydroxylamine oxidation. Results indicated that hydroxylamine peak potential at QMSNPs−GCE shifted for 170 and 260 mV to negative values compared to quinazolin−modified glassy carbon electrode (QMGCE) and silver nanoparticles coated glassy carbon electrode (SNPs−GCE) respectively. It was also shown that a combination of SNPs and modifier definitely improves the characteristics of hydroxylamine oxidation. The surface charge transfer rate constant, k_s, and the charge transfer coefficient, α, for electron transfer between GCE and electrodeposited quinazolin modified GCE were calculated as 39.5±1.1 s^{-1} and 0.53 respectively at pH=7.The electron transfer coefficient, α, and the heterogeneous rate constant, k′, for the oxidation of hydroxylamine at QMSNPs−GCE were also determined by cyclic voltammetry measurements. Furthermore, amperometric detection of hydroxylamine was carried out at 270 mV in a 0.1 M phosphate buffer solution (pH 7.0) resulting in two linear response ranges of 1.0−101.5 µM and 101.5−9410.8 µM and the limit of detection of 0.38 µM. Moreover, QMSNPs−GCE was successfully used to determine hydroxylamine in various water samples.

Keywords: Quinazolin, Hydroxylamine, ElectrocatalyticOxidation, Silver Nanoparticles, Self−Assembled monolayer layer.

1. INTRODUCTION

Nanomaterials have exhibited special properties that are differing from the bulk materials, originating from their quantum scale dimensions [1]. In recent years, nanomaterials of different forms,

have found wide applications in analytical methods [2−5]. Different kinds of nanomaterials, such as metals, metal oxides, semiconductor nanoparticles and carbon based materials have been used for fabricating electrochemical sensors and biosensors [6−9].

Among these nanomaterials, metallic nanoparticles have attracted much more attention in electro−analysis because of their excellent physical and chemical propertiessuch as large surface−to−volume ratio, good electrical properties, strong adsorption ability, high surface reaction activity, small particle size and good surface properties [10, 11]. The unique properties of metal nanoparticles make them highly suitable for designing and improving electrochemical sensors and biosensors [12]. Various nanoparticles such as Au, TiO_2, Pt, Cu, Pd, Ni and Ag were studies in the recent decades amongst them, silver nanoparticles (SNPs) attracted considerable interests because of their unique properties such as the capacitance character, excellent biocompatibility, good electrical conductivity and high catalytic activity [10, 13]. Recently, SNPs have gained in popularity and have been widely applied in construction of electrochemical sensors and biosensors [11, 14, 15]. For example Rounaghi et al. described the use of a crown ether and silver nanoparticle as modifiers in carbon paste electrodes for measurement of 4−nitrophenol [10]. Lian et al. developed an imprinted electrochemical sensor for neomycin recognition based on chitosan−silver nanoparticles (CS−SNP)/graphene−multiwalled carbon nanotubes (GR−MWCNTs) composites decorated gold electrode [11]. Zhou et al. fabricated a H_2O_2 biosensor based on the immobilization of sacrosine oxidase (SOX) on SNPs and graphene–chitosan composite film modified glassy carbon electrode (GCE) [13].

Self−assembled monolayers (SAMs) of S−functionalized compounds on metals were used in preparing chemical interfaces with stable and structurally well−defined monolayers [16]. Using SAMs to functionalize metal surfaces provides a simple route to functionalize electrode surfaces by organic molecules. Due to the high affinity of SH groups towards metals, thiol−terminated SAMs have attracted tremendous attention for construction of biomolecular electronic devices [17]. The materials used for the SAM preparation are Au [18], Cu [19], Pt [20], Pd [21], InP [22], GaAs [23] and Ag [24]. On the other hand, surface modifications using metallic nanoparticles could largely increase the immobilized amount of S−functionalized compounds and enhance stability of SAMs layer.

In the present work, we report the preparation of a thio−quinazolin derivative self−assembled layer on SNPs and application of this modified electrode as a new electrode for determination of hydroxylamine. The thio−quinazolin derivative was deposited on SNPs surface by self−assembling procedure. A new voltammetric sensing set−up was assembled using the fabricated electrode for studying the electrocatalytic oxidation of hydroxylamine. Cyclic voltammetry and amperometryhave been also used to investigate the electrochemical properties and electrocatalytic activity of the modified electrode for determination of hydroxylamine. In previous study, we reported the characteristics of a modified electrode prepared by electrodeposition of a thio−quinazoline derivative on the multi-wall carbon nanotubes modified glassy carbon electrode (QMWCNT-GCE) [25]. The charge transfer rate constant, k_s, was obtained 12.6±0.3 s^{-1} in pH 7.0 between thio−quinazoline and MWCNT−GCE. While in this work, k_s, is obtained 39.5±1.1 s^{-1} in pH 7.0 between thio−quinazoline and SNPs−GCE which this value of k_s is greater than obtained k_s at QMWCNT−GCE. The results

might confirm that the self−assembled layer of thio−quinazolin derivative on SNPs covered GCE improves the sensitivity, linear range, and detection limit of hydroxylamine determination.

2. EXPERIMENTAL

2.1. Materials and instrumental

Athio−quinazolin derivative, 2 − [(4, 5 – Dihydroxy – 2 − methylphenyl) thio] quinazolin − 4(3H) – one (see Scheme 1 for structure) was incorporated and purified in accordance to the method described before [26]. In the present paper, we revert to this derivative as quinazolin (Q) for simplicity. Silver nitrate, dimethyl formamide (DMF), hydroxylamine (NH_2OH), and the other chemical reagents used for preparation of the buffersolutions was analytical grades from Merck Companyand used as received.All the solutions were prepared with doubly distilled water. Hydroxylamine solutions were allprepared immediately prior to the useand all the experiments were carried out at room temperature. The phosphate buffer solution (0.1 M) was supplied with H_3PO_4 and the pH was adjusted using 2 M NaOH solution. All solutions tested were deaeratedby passing highlypure nitrogen (99.999%) before the electrochemicalexperiments.

An Autolab potentiostat−galvanostat PGSTAT 30 (Eco Chemie, Ultrecht, Netherlands) equipped with GPES 4.9 software, in connection with a three−electrode system and a personal computer was used for electrochemical measurements. The geometric area of quinazolin silver nanoparticles−modified glassy carbon working electrode (QSNPs−GCE) was 0.0314 cm^2. A platinum electrode (Azar Electrode Co, Iran) and a saturated calomel electrode (SCE) were used as the counter and reference electrodes respectively. All the potentials in the context are quoted versus this reference electrode. The pH measurements were done with a Metrohm model 827 pH/mV meters.

2.2. Electrodes preparation

Prior to modification, the bare glassy carbon electrode was polished consecutively with 0.05 μm Al_2O_3 slurry on apolishingcloth and then rinsed with doubly distilled water after each polishing step. Then, the electrode was consecutively inserted in 1:1 nitric acid, absolute ethanol and doubly distilled water in ultrasonic bath for 2 min. After being washed again with distilled water, the bare GCE (BGCE) was modified by acontinuous potentialcycling from–0.7 to 1.9 V at a sweep rate of 80 mV s^{-1} for 11 cycles in a solution containing 100 mM nitric acid and 1 mM $AgNO_3$ [27]. Finally, the modified electrode was rinsed with doubly distilled water and dried in air to give a silver nanoparticlesmodified GCE (SNPs−GCE).For the preparation of quinazolin−modified GCE (QMGCE), the BGCE was rinsed withdoubly distilled water and was modified by ten cycles ofpotential sweep between −0.5 and 0.8 Vat 20 mVs^{-1} in 1.0 mM solution of quinazolin in 0.1 M phosphate buffer (pH 7.0). The QMSNPs−GCE was prepared by the self−assembling technique, just by immersingthe SNPs−GCE in a 0.1 mM phosphate buffer solution(pH 7.0) containing 1.0 mM of quinazolin for 20 min without applying any potential to the electrode. After the formation of

quinazolin layer on SNPs−GCE surface, the modified electrodewas rinsedthoroughly with distilled water and was dipped into the buffersolution for testing its electrochemical behavior.

3. RESULTS AND DISCUSSION

3.1. Electrochemical behavior of QMSNPs−GCE

The cyclic voltammograms of a QMSNPs−GCE in a 0.1 M phosphate buffer (pH 7.0) at various scan rates are shown in Fig. 1.

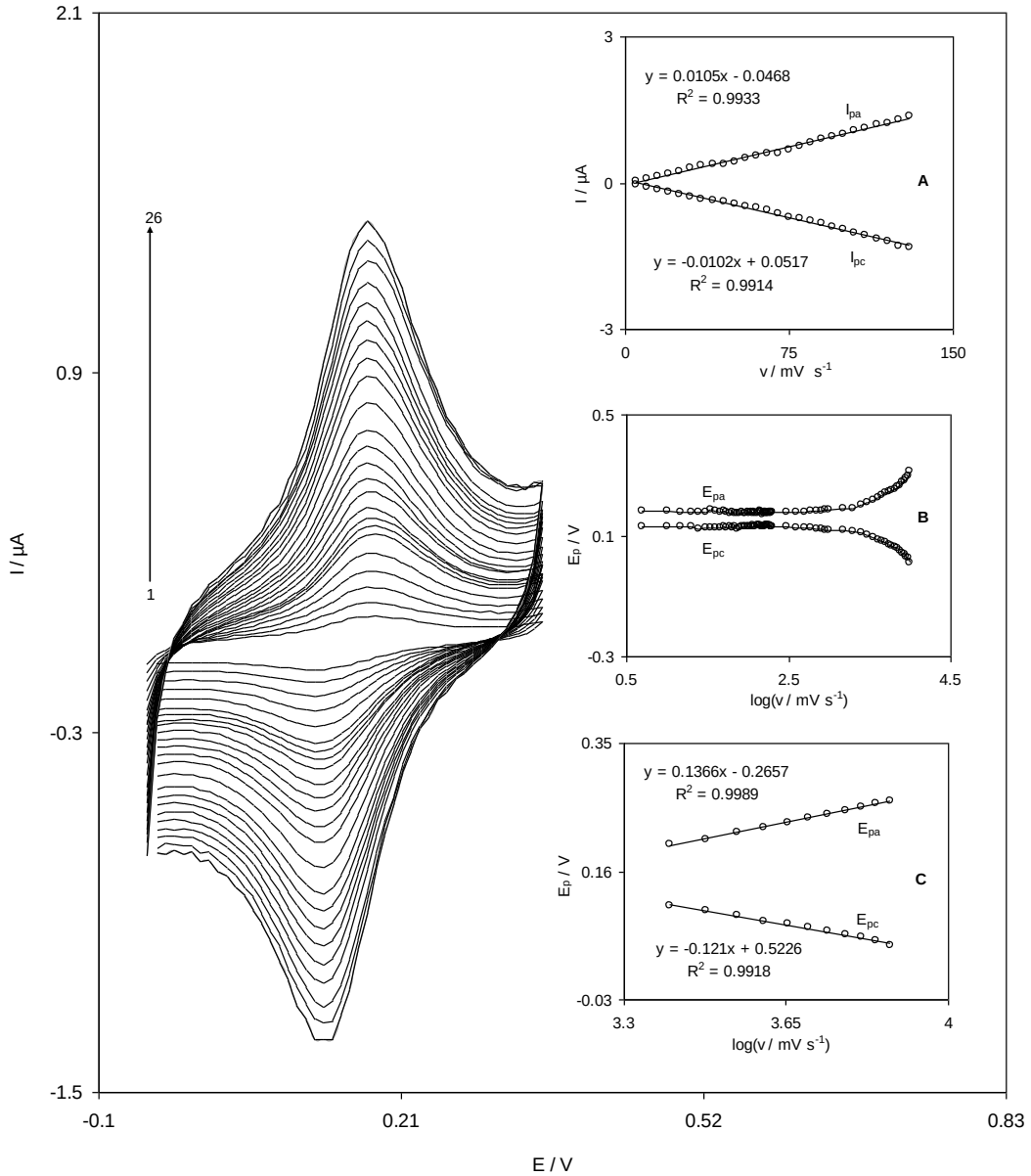

Figure 1. Cyclic voltammetric responses of QMSNPs−GCE in 0.1 Mphosphate buffer (pH 7.0) at different scan rates (5–130 mV s^{-1}). Insets: (A) plots of anodic andcathodic peak currents vs. of scan rate. (B) Variation of the peakpotentials vs. the logarithm of the scan rate. (C) Magnification of thesame plot for high scan rates.

The plots of the anodic and cathodic peak currents versus the scan rate exhibit a linear relation (Fig. 1A) as predicted theoretically for a surface−immobilized redox couple. In addition, the ratio of cathodic to anodic peak currents at various scan rates was almost constant. Moreover, because of the facility of charge transfer kinetics over the range of 5 to 1000 mV s^{-1}, the formal potential (E'_0) was almost independent of the potential scan rate for sweep rates at this range.

The formal potential (E'_0) value, which was obtained from the equation of $E^{0'}=E_{pa}-\alpha(E_{pa}-E_{pc})$ [28], is about 151 mV and for sweep rates ranging from 5 to 1000 mV s^{-1}. According to the method described by Laviron [29], the electron transfer coefficient, α, as well as the heterogeneous rate constant, k_s, for the charge transfer between the electrode and the surface confined redox couple can be calculated from the slope of variation of E_p versus log(V). Inset B of Fig. 1 shows the variations of peak potentials (E_p) as a function of the potential scan rate. The results show that the E_p values are proportional to the logarithm of the scan rate, for scan rates higher than 2500 mV s^{-1} (Fig. 1, inset C). Using the slope of plots in Fig. 1, inset C, the average values of α=0.53 and k_s=39.5±0.5 s^{-1} were obtained at pH 7.0. This value is greater than the previously reported values for other modifiers such as quinizarine (k_s=4.44 s^{-1}) [30], indenedione (k_s=2.3 s^{-1}) [31], and even caffeic acid (k_s=11.2 s^{-1}) [32]. Also, this value of k_s is greater than the value is obtained by QMWCNT−GCE in our previous work (k_s=12.6 s^{-1}) [25].

3.2. Electrochemistry of Hydroxylamine at QMSNPs−GCE

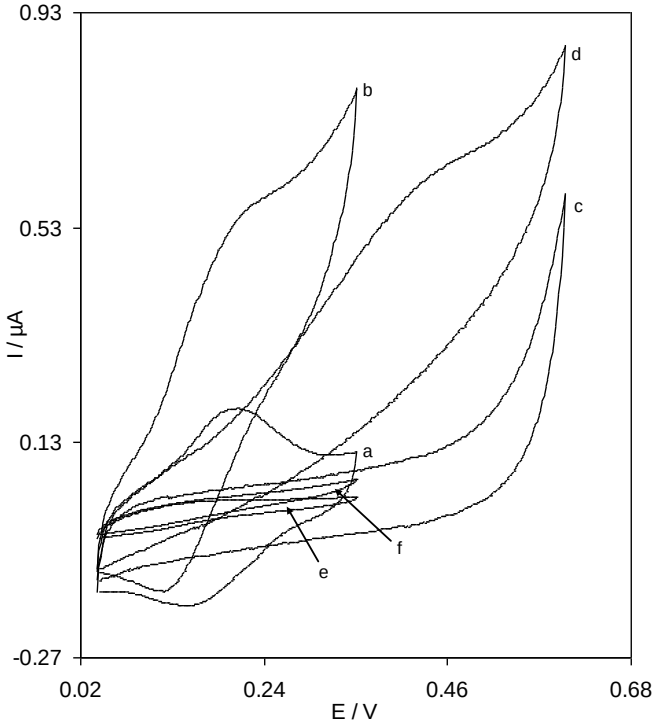

Figure 2. Cyclic voltammograms of QSNPs−GCE in 0.1 M phosphate buffer solution (pH 7) at scan rate 20 mVs^{-1} in the absence (a) and presence of 0.15 mM hydroxylamine (b). (c), (e) as (a) and (d), (f) as (b) for SNPs−GCE and bare GCE.

Table 1. Comparison of the electrocatalytic oxidation characteristics of hydroxylamine (0.15 mmol L^{-1}) on various electrode surfaces at pH 7.0

Type of electrode[a]	Oxidation peak potential / mV	Oxidation peak current / μA
SNPs−GCE	411	0.583
QMGCE	224	0.034
QSNPs−GCE	191	0.564

SNPs−GCE: silver nanoparticles modified glassy carbon electrode, QMGCE: quinazolin modified glassy carbon electrode, QMSNPs−GCE: quinazolin silver nanoparticles modified glassy carbon electrode.

In order to test the potential electrocatalytic activity of the quinazolin layer electrodeposited on GCE towards the oxidation of hydroxylamine, cyclic voltammograms of QMSNPs−GCE (Fig. 2, curves a), SNPs−GCE (Fig. 2, curves c), and QMGCE (Fig. 2, curves e) were obtained without and with 0.15 mM hydroxylamine. In absence of hydroxylamine, an excellent redox peaks couple of QMSNPs−GCE (curve a) can be observed**.** After addition of 0.15 mM of hydroxylamine, there is a noticeable intensification in the anodic peak currents and a small current is observed in the cathodic peak (Fig. 2, curves b). This behavior is related to a very strong electrocatalytic effect. According to the catalytic current responses shown in voltammograms b and f, this is anoticeableincrease in anodic peak current at QMSNPs–GCE (voltammogram b) compared to the value acquired from the QMGCE (voltammogram f). Actually, the higher current responses of QMSNPs–GCE observed as compared to QMGCE can be related to the increase in the surface area of QMSNPs–GCE. The electrocatalytic oxidation characteristics of hydroxylamine at various modified electrode surfaces at pH 7.0 are summarized in Table 1. Table 1, it is concluded that the best electrocatalytic effect for hydroxylamine oxidation is gained at QMSNPs−GCE surface.Also, the peak potential of hydroxylamine oxidation at QMSNPs−GCE (curve b) shifts by about 260 mV and 170 mV toward the negative values compared with that at a SNPs−GCE (curve d) and QMGCE (curve f), respectively. This means that, the combination of SNPs and a mediator (quinazolin) definitely improves the characteristics of hydroxylamine oxidation. The peak potential of hydroxylamine oxidation at the QMSNPs−GCE in majority of situations is less positive, compared to those reported for electrodes modified with other mediators such as caffeic acid [33], coumestan derinative [34], poly(acid yellow 9)/ nano−TiO_2 [35], rutin[36], hematoxylin [37], triazole [38], nickel hexacyanoferrate [39], an indenedione derivative [40] and ruthenium oxide nanoparticles [41]. The oxidation potentials reported for hydroxylamine on different modified electrodes are shown in Table 2 alongside with the value found in our work.

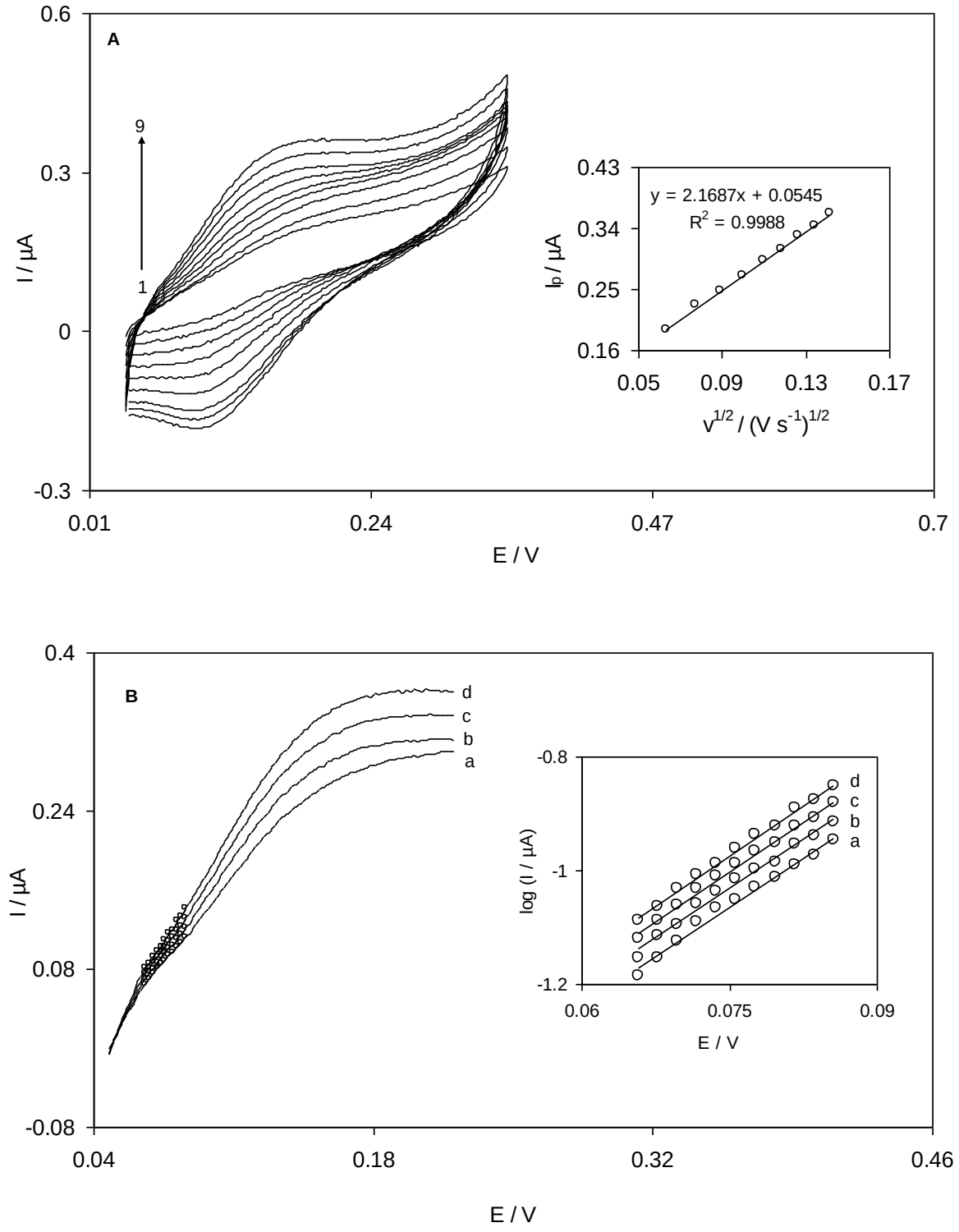

Figure 3. (A) Cyclic voltammograms of a QMSNPs−GCE in 0.1 M phosphate buffer solution (pH 7.0) containing 0.07 mM hydroxylamine. The numbers 1–9 correspond to scan rates of 4.0, 6.0, 8.0, 10.0, 12.0, 14.0, 16.0, 18.0 and 20.0 mV s^{-1}. Inset shows the variation of the electrocatalytic peak current vs. the square root of scan rate. (B) Linear sweep voltammograms of QMSNPs−GCE in 0.1 M phosphate buffer (pH 7.0) containing 0.07 mM hydroxylamine at scan rates of (a) 14 mV s^{-1}, (b) 16 mV s^{-1}, (c) 18 mV s^{-1} and (d) 20 mV s^{-1}. The points are the data used in the Tafel plots Inset shows the Tafel plots derived from linear sweep voltammograms.

Fig. 3A showsthe cyclic voltammograms of the QMSNPs−GCE at various scan ratesobtained in 0.1 M phosphate buffer solution (pH 7.0) containing 0.07 mM hydroxylamine. The peak current for the anodic oxidation of hydroxylamine is proportional to the square root of scan rate at 4 to 20 mV s^{-1} (inset of Fig. 3A). This result implies that, at a sufficient overpotential, the reaction is mass transport controlled while it is the best case for quantitative applications [42]. By this plot, the approximate total number of electrons in the overall reactioncan be calculated according to the following equationfor a totally irreversible diffusion controlled process [43]:

$$I_p=3.01\times10^5 n[(1-\alpha)n\alpha]^{1/2}AC_bD^{1/2}\nu^{1/2} \quad (1)$$

Where $D=4.11\times10^{-6}$ cm^2s^{-1} (diffusion coefficient of hydroxylamine obtained by chronoamperometry), $(1-\alpha)n_\alpha=0.69$, C_b is the bulk concentration of hydroxylamine (mol cm^{-3}), and A is the electrode surface area (0.0314 cm^2).

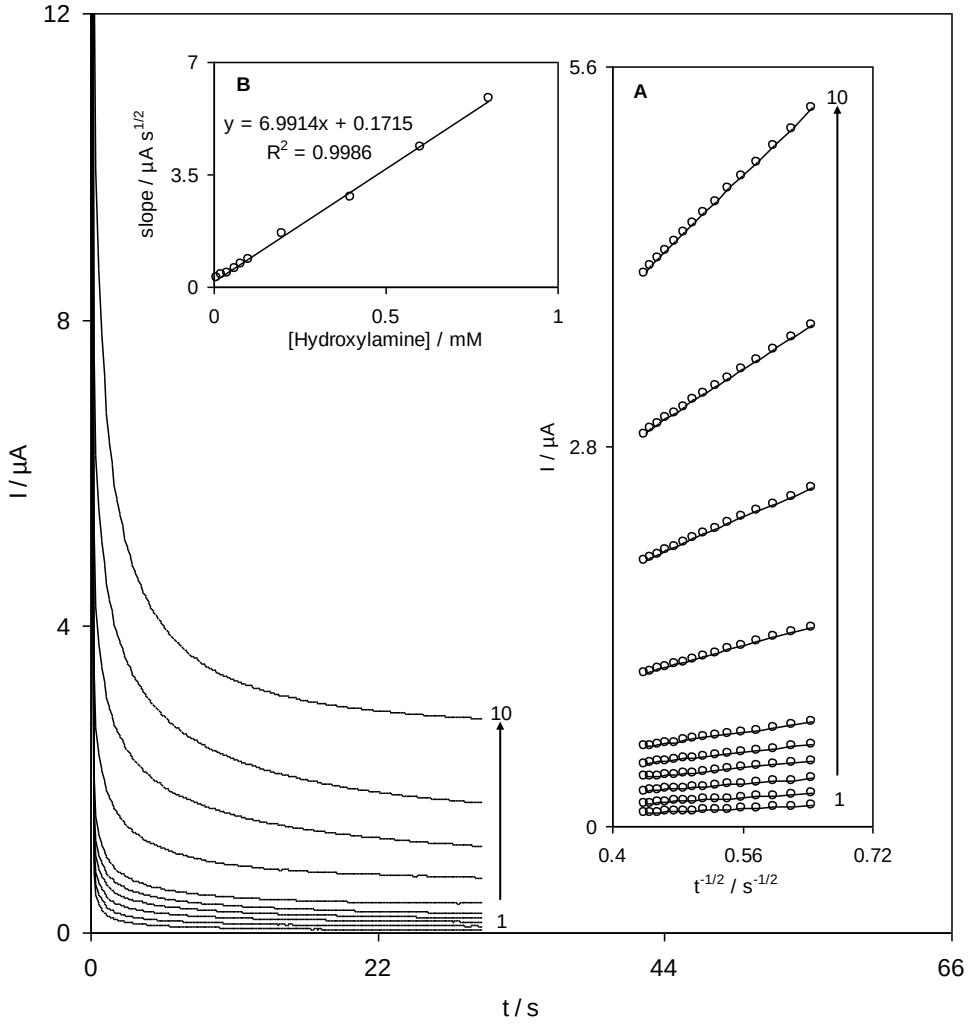

Figure 4. Chronoamperometric response at a QMSNPs−GCE in 0.1 Mphosphate buffer (pH 7.0) at a potential step of 270 mV for different concentrations of hydroxylamine. The numbers 1–10 correspond to 10.0, 20.0, 40.0, 60.0, 80.0, 100.0, 200.0, 400.0, 600.0, and 800.0 µM of hydroxylamine. Insets: (A) plots of I vs. $t^{-1/2}$ obtained from the chronoamperograms and (B) plot of the slope of the straight lines against the hydroxylamine concentration.

It is estimated that the total number of electrons involved in the anodic oxidation of hydroxylamine isn=1.94≅2. Based on the above results, one can describe the catalytic reaction (E_rC_i') mechanism of hydroxylamine at QMSNPs−GCE as shown in equations 2 and 3. For an E_rC_i' mechanism, Andrieux and Saveant theoretical model [44] can be used to calculate the catalytic rate constant between hydroxylamine and quinazolin, k′. According to the theoretical model of Andrieux and Saveant and using Fig. 4 in their paper [44], the average value of k′ was calculated to be $(1.2\pm0.03)\times10^{-3}$ cm.s^{-1}.

$$Quinazolin_{(red)} \underset{}{\overset{k_s}{\rightleftharpoons}} Quinazolin_{(ox)} + 2H^+ + 2e^- \quad (2)$$

$$2Quinazolin_{(ox)} + 2NH_2OH_2 \longrightarrow Quinazolin_{(red)} + N_2O + H_2O \quad (3)$$

The overall oxidation of hydroxylamine by the modified electrode is given in equation 4.

$$2NH_2OH \rightarrow N_2O + H_2O + 4H^+ + 4e^- \quad (4)$$

Linear sweep voltammograms of the modified electrode in a 0.1 M phosphate buffer solution (pH 7.0) containing 0.07 mM of hydroxylamine were obtained at different scan rates varying from 4 to 20 mV s^{-1} (Fig 3B). In order to evaluate information about the rate−determining step, Tafel plots were drawn (inset of Fig. 3B) from points of the Tafel region of the linear sweep voltammograms.The results of polarization studies for the electro−oxidation of hydroxylamine at QMSNPs−GCE show that, for all potential scan rates, the average of the anodic Tafel slopes of the different plots was obtained as11.6 V^{-1}. Referring to equation 5 [42], the mean Tafel slope of 11.6 V^{-1} concurs well with the involvement of one electron in the rate−determining step of electrode process, supposing a charge transfer coefficient of α=0.31.

$$\text{Tafel slope} = (1-\alpha)n_\alpha F/2.3RT \quad (5)$$

It is essential to mention that, in literatures, the number of electrons involved in the rate determining step of various processes is one. In addition, the exchange current density, J_0, is obviously readily accessible from the intercept of the Tafel plots. The average value of the exchange current density, J_0, for hydroxylamine oxidation at the modified electrode surface was found to be 0.5±0.01 μA.cm^{-2}. The value obtained for J_0 of hydroxylamine at QMSNPs−GCE is higher than the exchange current density at coumestan films (0.4 μA cm^{-2}) [34] but it is lower than the J_0 value of hydroxylamine at oracet blue films (2.4 μA cm^{-2}) [40].

3.3. Chronoamperometric studies

The catalytic oxidation of hydroxylamine by a SNPs modified glassy carbon electrode was investigated bychronoamperometry technique in which, the diffusion coefficient of NH_2OH was

determinedat the sensor surface. The chronoamperograms of the QMSNPs−GCE in 0.10M phosphate buffer (pH 7.0) including different concentrations of NH_2OH obtained at a potential step of 270 mV are shown in Fig. 4. For an electroactive material (hydroxylamine) with a diffusion coefficient, D, the current corresponding to the electrochemical reaction (under diffusion control) is delineated by Cottrell equation [42]:

$$I=nFAD^{1/2}C/\pi^{1/2}t^{1/2} \quad (6)$$

where D and C are the diffusion coefficient (cm^2s^{-1}) and bulk concentration ($mol.cm^{-3}$) of the analyte respectively. Fig. 4A, shows the tentative plots of I against$t^{-1/2}$ for different concentrations of hydroxylamine employed in the experiments. The slopes of the resulting straight lines were then plotted versus the hydroxylamine concentration (inset B) which from its slope we found a diffusion coefficient of 4.11×10^{-6} cm^2s^{-1} for hydroxylamine. The calculated diffusion coefficient is in a good consent with that previously reported values obtained for hydroxylamine [43].

3.4. Amperometric detection of hydroxylamine at a QMSNPs−GCE

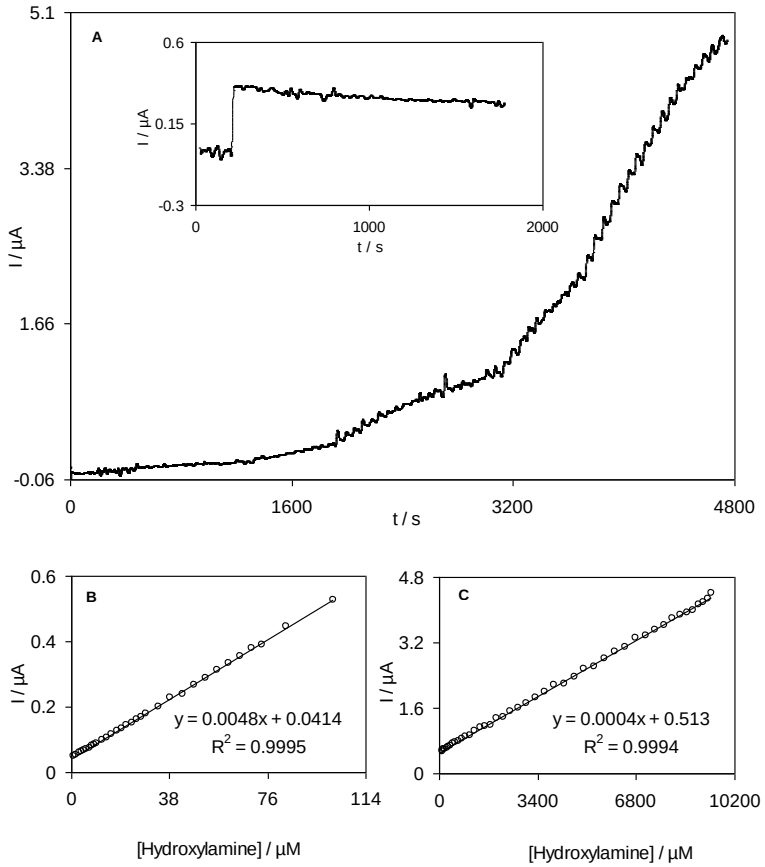

Figure 5. (A) Amperometric responses at a rotating QMSNPs−GCE (rotation speed 2000 rpm) held at 270mV in different concentrations of 1.0−9410.8 µmol L^{-1}hydroxylamine. Inset shows the stability of the response of QMSNPs−GCE to 60 µM hydroxylamine during 1776 s. (B) and (C) showvariations of the amperometric currents *vs*. hydroxylamine concentrations in the two ranges of 1.0−101.5 µmol $L^{-1}$and 101.5−9410.8 µmol L^{-1}.

Amperometry under stirred condition has a much higher current sensitively than cyclic voltammetry and it can be used for determination in the linear range and to estimate the lowest limit of detection of hydroxylamineby a QSNPs−GCE. Fig. 5A shows amperograms which were recorded for a rotating QSNPs−GCE (rotation speed 2000 rpm), under conditions where the potential was held at 270 mV in different concentrations of 1.0−9410.8 μM of hydroxylamine. As shown in Fig. 5, even at very low concentrations such as 1.0 or 10.0 mM of hydroxylamine, very niceand specific responses can be observed in amperograms. After each step of addition of hydroxylamine, a sharp rise in the current was perceived within a response time less than 2 seconds. Also, Fig. 5B and 5C clearly show that the plot of the peak current against the hydroxylamine concentration is formed of two linear segments of 1.0−101.5 and 101.5−9410.8 μM with different slopes. In accordance with the procedure reported in the reference [44], the lower limit of detection, C_m, was procured to be 0.38 μM by utilizing the equation $C_m=3s_{bl}/m$, where s_{bl} is the standard deviation of the blank response and m is the slope of the calibration plot in the confine of 1.0−105.5 μM of hydroxylamine (0.0048 μA μM^{-1}).

Table 2. Comparison of the analytical parameters of the hydroxylamine oxidation at various modified electrode surfaces

Modifier electrode	Linear range (μM)	Sensitivity (μA μM)	Limit of detection (μM)	Ref
Caffeic acid	2.5−1000	3.16	0.40	[33]
A coumestan derivative	1.0−40.0	6.10	0.61	[34]
Poly(acid yellow 9)/nano−TiO_2	12.0−120.0	−	2.0	[35]
Rutin MWCNT	1.0−33.8 33.8−81.7	0.0228 0.025	1.0	[38]
Triazole	0.10−10.0 10.0−600.0	0.083	0.01	[38]
Hematoxylin	2.0−122.8	0.0208	0.68	[37]
Nickel hexacyanoferrate	1.0−50.0	0.0046	0.024	[39]
Indenedione derivative	1.0−10.0 10.0−100.0	0.1955 0.0841	0.8	[40]
QMSNPs−GCE	1.0−101.5 101.5−9410.8	0. 0048 0.0004	0.38	This work

In table 2, the analytical parameters of electrocatalytic determination of hydroxylamine in this work are compared with the corresponding values previously reported for some other modified electrodes [33−40]. It can be seen that the responses observed for this modified electrode in most cases are better than responses obtained from previously reported modified electrodes. The average current and the measurement precision shown by the relative standard deviation (RSD %) innine repeated measurements (n=9) of an aqueous sample containing 10.0 mM of hydroxylamine at the applied potential of 270 mV on QMSNPs−GCE were measured as 0.09±0.002 μA and 2.2% respectively. The amperometric response of a 60 μM solution of hydroxylamine over a period of 1776 s (inset of Fig.

5A) indicates that after an initiatory decline of current, the response of QMSNPs−GCE has remained almost stable during the whole experiment. It seems to be logical to conclude that there is no suppressive effect of hydroxylamine and its oxidation product (s) on the modified electrode surface. Hence QMSNPs−GCE was found to have outstanding aadvantages such ashigh sensitivity, fast response time, a good limit of detection and a comprehensive linear range for hydroxylamine determination.

The utility of the present hydroxylamine sensor for the determination of hydroxylamine in real samples was tested by measuring hydroxylamine in two water samples. In order to run the test, 3 ml of fresh water sample was diluted to 10 mL with a 0.1 M phosphate buffer solution (pH 7.0). Then, definite amounts of hydroxylamine were added and responses of the sensor having QMSNPs−GCE as working electrode were determined in amperometric measurements. The measurements were done using the calibration plots shown in the Fig. 5B. The results are summarized in Table 3.

Table 3. Determination of hydroxylamine concentration in two water samples with QMSNPs−GCE.

Samples	Added (μM)	Found (μM)	RSD (%)	Recovery %
Well water	–	Not found	–	–
	25.00	24.82	2.6	99.3
	50.00	51.05	2.1	102.1
Tap water	–	Not found	–	–
	30.00	30.51	3.0	101.7
	60.00	59.10	2.3	98.5

The results that were obtained by the amperometric technique showed satisfactory recovery, demonstrating that the QMSNPs−GCE could be efficiently used in practical applications.

4. CONCLUSIONS

This work demonstrated that a new quinazolin derivative can be immobilized easily on the surface of silver nanoparticles (SNPs) modified glassy carbon electrode (GCE).The results show that the reversibility of quinazolin and its electrocatalytic activity for hydroxylamine oxidation are significantly improved when a QMSNPs−GCE is used instead of QMGCE or SNPs−GCE.According to the data in this study, the diffusion coefficient of hydroxylamine was determined as 4.11×10^{-6} cm^2s^{-1} for experimental conditions using chronoamperometric results. In amperometric measurements, a limit of detection of 0.38 μM and two linear ranges has been obtained for hydroxylamine at the proposed modified electrode. Technical simplicity, high sensitivity, low detection limit and wide linear

concentration ranges for hydroxylamine are the great advantages of the newly introduced modified electrode. Finally, it has emerged that amperometric method can be used as an analytical method to determine hydroxylamine in two water samples using the proposed modified electrode.

References

1. X. Tian, C. Cheng, H. Yuan, J. Du, D. Xiao, S. Xie and M. Choi, *Talanta*, 93 (2012) 79.
2. S. Prakash, T. Chakrabarty, A. K. Singh and V. K. Shahi, *Electrochim. Acta.,* 72 (2012) 157.
3. S. Prakash and V.K. Shahi, *Anal. Met.,* 3 (2011) 2134.
4. R. S. Babu, P. Prabhu and S. S. Narayanan, *Talanta*, 110 (2013) 135.
5. T.G.S. Babu and T. Ramachandran, *Electrochim. Acta.,* 55 (2010) 1612.
6. H. Gao, X. Qi, Y. Chen and Wei Sun, *Anal. Chim. Acta.,* 704 (2011) 133.
7. N.N. Zhu, Y.Q. Lin, P.Yu, L.Suand L.Q. Mao, *Anal. Chim. Acta.,* 650 (2009) 44.
8. J. Liu, X. Yuan, Q. Gao, H. Qi and C. Zhang, *Sens. Actuators. B,* 162 (2012) 384.
9. G.J. Li, X.L. Li, J. Wan and S.S. Zhang, *Biosens. Bioelectron.,* 24 (2009) 3281.
10. G. Rounaghi, R. Mohamadzadeh−kakhki and H. Azizi−toupkanloo, *Mater. Sci. Eng*. C, 32 (2012) 172.
11. W. Lian, S. Liu, J. Yu, J. Li, M. Cui, W. Xu and J. Huang, *Biosens. Bioelectron.,* 44 (2013) 70.
12. M. Arvand, R. Motaghed−Mazhabi and A. Niazi, *Electrochim. Acta.,* 89 (2013) 669.
13. Y. Zhou1, H. Yin, X. Meng, Z. Xu, Y. Fu and S. Ai, *Electrochim. Acta.,* 71 (2012) 294.
14. H. Quan, S. U. Park and J. Park, *Electrochim. Acta.,* 55 (2010) 2232.
15. YShi,Z.L. Liu, B. Zhao, Y. J. Sun, F. G. Xu, Y.Zhang,Z. W.Wen,H. B.Yang and Z. Li, *J.Electroanal. Chem.,* 656 (2011) 29.
16. T. Luczak, *Electrochim. Acta.,* 54 (2009) 5863.
17. M. Mazloum−Ardakani, H. Beitollahi, M. K. Amini, B. F. Mirjalili and F.Mirkhalaf, *J. Electroanal. Chem.,* 651 (2011) 243.
18. J. Jiao, H. Zhang, L. Yu, X. Wang and R. Wang, *Colloids Surfaces A,* 408 (2012) 1.
19. C. M. Whelan, M. Kinsella, L. Carbonell, H. M. Ho, K. Maex, *Microelectron. Eng.,* 70 (2003) 551.
20. B. Y. Wu, S. H. Hou, F. Yin, Z. X. Zhao, Y. Y. Wang, X. S. Wang and Q. Chen, *Biosens. Bioelectron.,* 22 (2007) 2854.
21. W.L. Wang, Y.Y. Wang, C.C. Wan and C.L. Leev, *Colloids Surfaces A,* 275 (2006) 11.
22. J. Lefebvre, P.J. Poole, J. Fraser, G.C. Aers, D. Chithrani and R.L. Williams, J. *Cryst. Growth,* 234, 2002, 391−398.
23. A. Aierken, T. Hakkarainen, M. Sopanen, J. Riikonen, J. Sormunen, M. Mattila and H. Lipsanen, *Appl. Surf. Sci.,* 254 (2008) 2072.
24. H. Yang, Y. Yang, Z. Liu, Z. Zhang, G. Shen and R. Yu, *Surf. Sci*., 551 (2004) 1.
25. M. M. Aghayizadeh, N. Nasirizadeh, S. M. Bidoki and M. E. Yazdanshenas, *Int. J. Electrochem. Sci.,* 8 (2013) 8848.
26. A. R. Fakhari, K. Hasheminasab, H. Ahmar and A. A. Alizadeh, *Synthesis*, 24 (2008) 3963.
27. M. Chao and X. Ma *Int. J. Electrochem. Sci.,* 7 (2012) 6331
28. H. Ju andC. Shen, *Electroanalysis,* 13 (2001) 789.
29. E. Laviron *J. Electroanal. Chem.,* 101 (1979) 19.
30. M.Mazloum−Ardakani, P. Ebrahimi−Karami,H. Naeimi and B.F Mirjalili, *Turk. J. Chem.,* 32 (2008) 571
31. H. R. Zare, N. Nasirizadeh, F. Chatraei and S. Makarem *Electrochim. Acta.,* 54 (2009) 2828.
32. H.R. Zare and S.M. Golabi, *J. Solid State Electrochem.,* 4 (2000) 87.
33. S. M. Golabi andH. R. Zare, *Electroanalysis*, 11 (1999) 1293.
34. H. R. Zare andA. M Habibirad, *J. Solid State Electrochem.,* 10 (2006) 348.
35. H. R. Zarea and N. Nasirizadeh, *Int. J. Electrochem. Sci.,* 4 (2009) 1691.

36. H. R. Zare, Z. Sobhani and M. Mazloum−Ardakani, *Sens. Actuators.B,* 126 (2007) 641.
37. H. R. Zare and N. Nasirizadeh,*Electrochim. Acta.,* 52 (2007) 4153.
38. J.A. Ni, H.X. Ju, H.Y. Chen and D. Leech, *Anal. Chim. Acta.*, 378 (1999) 151.
39. A. Salimi, K. Abdi, *Talanta,* 63 (2004) 475.
40. H. R. Zare and Navid Nasirizadeh, J. *Braz. Chem. Soc.,* 23 (2012) 1070.
41. H. R. Zare, S. H. Hashemi, A. Benvidi, *Anal. Chim. Acta.*, 668 (2010) 182.
42. A. J. Bard, L. R. Faulkner, Wiley. New York, (2001).
43. S. Antoniadou, A. Jannakoudakis, E. Theodoridou, *Synth. Met.,* 30 (1989) 295.
44. C. P. Andrieux, J. M. Saveant, *J. Electroanal. Chem.,* 93 (1978) 163.